Accepted Manuscript

N-(4-[18F]fluorobenzyl)cholylglycine, a novel tracer for PET of enterohepatic circulation of bile acids: Radiosynthesis and proof-of-concept studies in rats

Kim Frisch, Damion H.R. Stimson, Taracad Venkatachalam, Gregory K. Pierens, Susanne Keiding, David Reutens, Rajiv Bhalla
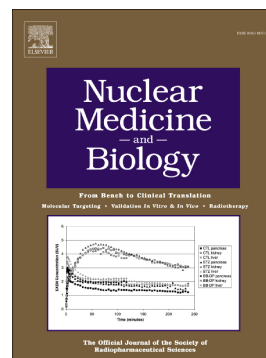
Please cite this article as: Kim Frisch, Damion H.R. Stimson, Taracad Venkatachalam, Gregory K. Pierens, Susanne Keiding, David Reutens, Rajiv Bhalla , N-(4-[18F]fluorobenzyl)cholylglycine, a novel tracer for PET of enterohepatic circulation of bile acids: Radiosynthesis and proof-of-concept studies in rats. The address for the corresponding author was captured as affiliation for all authors. Please check if appropriate. Nmb(2018), doi:10.1016/j.nucmedbio.2018.04.004

N-(4-[^{18}F]fluorobenzyl)cholylglycine, a novel tracer for PET of enterohepatic circulation of bile acids: radiosynthesis and proof-of-concept studies in rats

Kim Frisch[1], Damion H. R. Stimson[2], Taracad Venkatachalam[2], Gregory K. Pierens[2], Susanne Keiding[1,3], David Reutens[2], Rajiv Bhalla[2].

[1] *Department of Nuclear Medicine & PET Centre, Aarhus University Hospital, Aarhus, Denmark;* [2] *Centre for Advanced Imaging, University of Queensland, St. Lucia, Brisbane, Australia;* [3] *Department of Hepatology & Gastroenterology, Aarhus University Hospital, Aarhus, Denmark.*

Corresponding Author:

Kim Frisch, Department of Nuclear Medicine and PET Centre, Aarhus University Hospital, DK-8000 Aarhus C, Denmark. Phone: +45 7846 3031; E-mail: kimfrisc@rm.dk

Abbreviated Title: [^{18}F]FBCGly PET of enterohepatic circulation

Key Words: Bile acids; Bile salt export pump; Enterohepatic circulation; Fluorine-18 labelling; Metabolism; Positron emission tomography

Abstract

Introduction: Enterohepatic circulation (EHC) of conjugated bile acids is an important physiological process crucial for regulation of intracellular concentrations of bile acids and their function as detergents and signal carriers. Only few bile acid-derived imaging agents have been synthesized and hitherto none have been evaluated for studies of EHC. We hypothesized that *N*-(4-[^{18}F]fluorobenzyl)cholylglycine ([^{18}F]FBCGly), a novel fluorine-18 labeled derivative of endogenous cholylglycine, would be a suitable tracer for PET of the EHC of conjugated bile acids, and we report here a radiosynthesis of [^{18}F]FBCGly and a proof-of-concept study by PET/MR in rats.

Methods: A radiosynthesis of [^{18}F]FBCGly was developed based on reductive alkylation of glycine with 4-[^{18}F]fluorobenzaldehyde followed by coupling to cholic acid. [^{18}F]FBCGly was investigated *in vivo* by dynamic PET/MR in anaesthetized rats; untreated or treated with cholyltaurine or rifampicin. Possible *in vivo* metabolites of [^{18}F]FBCGly were investigated by blood and bile sampling, and the stability of [^{18}F]FBCGly towards enzymatic de-conjugation by Cholylglycine Hydrolase was tested *in vitro*.

Results: [^{18}F]FBCGly was produced with a radiochemical purity of 96% ± 1% and a non-decay corrected radiochemical yield of 1.0% ± 0.3% (mean ± SD; *n* = 12). PET/MR studies showed that i.v.-administrated [^{18}F]FBCGly underwent EHC within 40–60 min with a rapid transhepatic transport from blood to bile. In untreated rats, the radioactivity concentration of [^{18}F]FBCGly was approximately 15 times higher in bile than in liver tissue. Cholyltaurine and rifampicin inhibited the biliary secretion of [^{18}F]FBCGly. No fluorine-18 metabolites of [^{18}F]FBCGly were observed.

Conclusion: We have developed a radiosynthesis of a novel fluorine-18 labeled bile acid derivative, [^{18}F]FBCGly, and shown by PET/MR that [^{18}F]FBCGly undergoes continuous EHC in rats without metabolizing. This novel tracer may prove useful in PET studies on the effect of drugs or diseases on the EHC of conjugated bile acids.

1. Introduction

The formation of bile acids in the liver and their secretion into bile canaliculi and onwards into the small intestine play an essential role in digestion and detoxification, and in metabolic signaling [1-3]. Before secretion from hepatocytes, bile acids are conjugated (*N*-acyl amidated) with glycine or taurine. Less than 10% of the secreted bile acids stem from *de novo* synthesis; the rest have undergone enterohepatic circulation (EHC), i.e. the continuous circulation of bile acids between liver and small intestine [1, 2, 4]. The EHC, which occurs 6–10 times per day in humans [5], results from active vectorial transport of bile acids across hepatocyte and enterocyte membranes, and involves several transporter proteins [6]. These proteins include the Bile Salt Export Pump (BSEP), which accounts for the rate-limiting step of the overall transport across the hepatocyte [7], and the Apical Sodium-dependent Bile acid Transporter (ASBT), which is located mainly in ileal enterocytes and accounts for more than 90% of the absorption of bile acids from the intestinal lumen [8, 9]. The EHC ensures optimal concentrations of bile acids at the sites of their physiologic actions and hence allows bile acids to form micelles and dissolve digested lipids in the small intestine and to function as signal molecules, while keeping the intracellular concentration of bile acids low to avoid cellular damages [1, 10]. Several factors may perturb the EHC and lead to liver and gastrointestinal disorders [2, 11-13]. Cholestatic liver diseases and drug-induced inhibition of BSEP result in accumulation of bile acids in hepatocytes, which leads to liver injury, treatable only by liver transplantation in severe cases [7, 14]. Impaired intestinal uptake caused by lack of the ileum or by drug-induced inhibition of ASBT results in bile acid malabsorption and excessive excretion of bile acids to the colon, which leads to severe diarrhea, alteration of the gut microbiome and, potentially, development of colorectal cancer [13].

A method for non-invasive quantitative imaging of the dynamic EHC of conjugated bile acids *in vivo* would be a valuable tool for investigations of the underlying pathological mechanisms of diseases that affect the EHC and of drugs inhibiting hepatic and intestinal transport of conjugated bile acid.

3

The development of such method is likely to be successful only if the imaging agent is derived from an endogenous bile acid conjugate, since these are the only molecules that so far have been shown to go through all features of the EHC [10]. The current standard of practice for quantification of the EHC do involve an analog, 23-[^{75}Se]seleno-25-homotaurocholic acid, closely related to endogenous cholyltaurine, but the method provides only a measure of the retention of the labeled analog in the body; not quantifiable images of its circulation between liver and ileum [15]. Other labeled bile acid analogs have been investigated for single photon emission computed tomography [16], magnetic resonance [17-19], and PET imaging [20-26], but so far no imaging agent has been reported for imaging of the EHC. In particular, [^{11}C]cholylsarcosine, a carbon-11 labeled analog of endogenous cholylglycine [20], has proven useful for quantification of hepatic transport of conjugated bile acids in healthy persons and in patients with cholestatic liver disease by PET/CT [27, 28]. However, although cholylsarcosine is known to undergo EHC, the use [^{11}C]cholylsarcosine as PET tracer for EHC is limited by the relatively short half-life of the carbon-11 radioisotope (^{11}C; $T_{\frac{1}{2}}$ = 20.3 min). We therefore set out to develop a novel bile acid tracer with properties comparable to [^{11}C]cholylsarcosine, but labeled with a positron emitting isotope with a radioactive half-life suitable for studies of EHC. Here we report a radiosynthesis of *N*-(4-[^{18}F]fluorobenzyl)cholylglycine ([^{18}F]FBCGly), a novel fluorine-18 (^{18}F; half-life = 109.8 min) labeled derivative of endogenous cholylglycine, and show in a proof-of-concept study in rats that [^{18}F]FBCGly is a PET tracer for EHC.

2. Materials and methods

2.1 General information

Chemicals and solvents were obtained from Sigma-Aldrich or VWR International Ltd and used as received. Water was sterile or MilliQ water. Cholylglycine Hydrolase from *Clostridium perfringens* (*C. welchii*) (lyophilized powder, ≥100 units/mg) was obtained from Sigma-Aldrich. Cholylglycine-2,2,4,4-d_4 was obtained from CDN Isotopes. (4-Formylphenyl)trimethylammonium triflate [29] and unlabeled cholylsarcosine [20] were prepared as described in the literature. 4-Fluorobenzylalcohol (used for identification purposes only) was prepared by reduction of 4-fluorobenzaldehyde with sodium borohydride in methanol. Unlabeled *N*-(4-fluorobenzyl)glycine methyl ester (FBGly-ME), *N*-(4-fluorobenzyl)cholylglycine methyl ester (FBCGly-ME), and *N*-(4-fluorobenzyl)cholylglycine (FBCGly) were prepared and characterized (^{1}H, ^{13}C, ^{19}F, COSY, HSQC, HMBC and ROESY NMR) as described in Supplementary Material. For comparison, NMR spectra of cholic acid are also reported. Sep-Pak® Accell Plus QMA Carbonate Plus Light Cartridge (130 mg sorbent/cartridge, 37–55 μm particle size) and Sep-Pak® Alumina N Plus Light Cartridges (280 mg sorbent/cartridge, 50–300 μm particle size) were obtained from Waters® and used as received. Sep-Pak® C_8 Plus Short Cartridges (400 mg sorbent/cartridge, 37–55 μm particle size), also obtained from Waters®, were conditioned before use with 10 mL ethanol, then 10 mL water, and finally 10 mL air.

2.2 Radiochemistry

The developed radiosynthesis of [^{18}F]FBCGly is illustrated in Fig. 1. No-carrier-added [^{18}F]fluoride was produced by the ^{18}O(p,n)^{18}F nuclear reaction from irradiation of isotopically enriched [^{18}O]H$_2$O (Rotem Industries, Deer Sheva, Israel) using a cyclotron (GE PETtrace 16.4-MeV proton beam or IBA Cyclone 18/18). The [^{18}F]fluoride (40–60 GBq) was trapped on a QMA cartridge and eluted into a 3 mL reaction vessel with a solution of K222 (Kryptofix™; 5 mg; 13 μmol) and K$_2$CO$_3$ (0.7 mg ; 5 μmol) in a mixture of water (0.30 mL) and acetonitrile (0.30 mL). The [^{18}F]fluoride was dried in the reactor by azeotropic distillation from anhydrous acetonitrile (3x0.6 mL) under a stream of helium at 120 °C. The temperature was lowered to 80

5

^{o}C, a solution of (4-formylphenyl)trimethylammonium triflate (2 mg; 6 µmol) in anhydrous

dimethylsulfoxide (0.3 mL) was added, and the mixture was heated at 105 ^{o}C for 10 min. The crude [^{18}F]FBA

(dark orange to brown in color) was purified by passing it through an alumina N cartridge, which was

subsequently washed with anhydrous dimethylsulfoxide (0.2 mL), into a second 3 mL reaction vessel. A

solution of glycine methyl ester hydrochloride (2 mg; 16 µmol) and triethylamine (3 µL; 22 µmol) in

anhydrous dimethylsulfoxide (0.1 mL) was added to the purified [^{18}F]FBA and the mixture was heated at 60

^{o}C for 10 min. The reaction vessel was cooled to 25 ^{o}C using a stream of cold air, a solution of NaBH$_4$ (2 mg;

53 µmol) in anhydrous dimethylsulfoxide (0.1 mL) was added, and the mixture was allow to stand for 5 min.

A solution of cholic acid (16 mg; 39 µmol) and triethylamine (9 µL; 65 µmol) in anhydrous dimethylsulfoxide

(0.1 mL) was added, followed by a solution of diethyl phosphoryl cyanide (12 µL; 79 µmol) in anhydrous

dimethylsulfoxide (0.1 mL). The temperature was raised to 60 ^{o}C and the mixture was heated for 10 min. All

added solutions were freshly prepared. After cooling to 25 ^{o}C, the reaction mixture was diluted with water

(9 mL) and [^{18}F]FBCGly-ME was trapped on a conditioned C$_8$ cartridge. The cartridge was washed with water

(10 mL) and 50% aqueous ethanol (10 mL), and eluted with 100% ethanol (1 mL) into a product vial.

Aqueous NaOH (2 mL; 0.25 N) was added to the product vial and the mixture was allowed to stand at room

temperature for 10 min with occasional shaking. The basic mixture was finally neutralized with aqueous

NaH$_2$PO$_4$ (7 mL; 70 mM). Total synthesis time was 90 min from delivery of [^{18}F]fluoride.

The product formulation of [^{18}F]FBCGly was analyzed by reverse-phase HPLC with a PDA-detector (Dionex

Ultimate® 3000 system) connected in series with a gamma-detector (Gabistar; Nuclear Interface) and an ESI

mass spectrometer (Bruker Daltonics HCT Plus ion trap mass spectrometer) running in negative ionization

mode. The column was a Phenomenex® Luna® 5µ C18(2) 100A (5 µm, 150x4.6 mm) with an isocratic eluent

of 50% acetonitrile in aqueous 1 mM NH$_4$OAc (pH 3.0; adjusted with glacial acetic acid) and a flow of 1

mL/min. The product formulation of [^{18}F]FBCGly was also tested for free [^{18}F]fluoride by radio-iTLC

(Supplementary Material). The identity of [^{18}F]FBCGly (retention time: 8.2 min) was confirmed by co-

injection of unlabeled reference material by monitoring its UV (254 nm) and MS (572.3 m/z) signals. For determination of molar radioactivity, the amount of FBCGly was determined by MS using a series of standard solutions (2, 5, 10, and 20 µg/mL) and with cholylglcyine 2,2,4,4-d_4 as internal standard. To investigate the individual steps of the radiosynthesis, the formation of reaction intermediates was analyzed by radio-HPLC (Supplementary Material).

2.3 In vivo PET/MR and metabolite studies

All animal experiments were carried out at the Dept. of Nuclear Medicine & PET Centre, Aarhus University Hospital, Aarhus, Denmark. The animal experiments were performed according to the Danish Animal Experimentation Act and the European convention for the protection of vertebrate animals used for experimental and other purposes (European Treaty Series no. 123). Prior to the experiments, female Sprague-Dawley rats (*n* = 10; 208 – 333 g) were kept in a temperature and light-controlled environment and provided with standard food and water *ad libitum*. For the duration of the experiments, the animals were positioned on the heat-controlled (37 $^{\circ}$C) bed and kept under general anesthesia with 2% isoflurane (IsoFlo® vet 100%, Zoetis) in air (1.5 L/min atmospheric air and 0.5 L/min O_2). [^{18}F]FBCGly was administrated as a single bolus (19–35 MBq) through a 24 GA venflon (Neoflon, Becton Dickinson) in the tail vein. After completion of the experiments, the animals were euthanized with an overdose of sodium pentobarbital (Euthanimal, 400 mg/mL, Alfasan).

PET/MR imaging of Rats 1–7 were performed using a small-animal PET/MR scanner (nanoScan, Mediso) with a transaxial PET field of view of 12 cm and a permanent 1 Tesla magnet for MR. Rats 1–3 were injected with [^{18}F]FBCGly only, while Rat 4 and Rat 5 were co-injected with cholyltaurine (68 mg/kg) simultaneous with the tracer. Rat 6 and Rat 7 were given a constant infusion of rifampicin (2 mg/kg/min) in isotonic saline initiated 40 min before the start of the PET scan and maintained throughout the scan. PET scans were acquired in 3D list-mode for 120 minutes with the field of view of the PET camera covering abdomen and

the lower part of thorax. MR scans were recorded for definition of anatomic structures (T1 weighted) and for attenuation and scatter correction of the PET recordings. PET recordings were obtained with the energy window set to 400–600 keV. Corrections for dead-time, radioactivity decay, attenuation, random and scatter counts were done using the manufacturer' software. The dynamic images were obtained by sorting the list mode data into the following time frames: 8x15, 4x30, 2x60, 2x120, 4x300, and 9x600 sec. The images were reconstructed with an algorithm (Tera-Tomo 3D; median filtering period: iteration count) provided by the manufacturer. Volumes-of-interest for liver tissue (excluding large blood vessels and visible intrahepatic bile ducts) and bile duct were manually drawn using the PMOD software (PMOD Technologies) and used to generate time courses of radioactivity concentrations (reported as %ID/mL tissue vs. min, where ID is percent of injected dose). The radioactivity concentrations were decay corrected to the start of the scan.

Rats 8–10 were investigated for possible *in vivo* metabolites of [^{18}F]FBCGly. For Rat 8 and Rat 9, blood samples were collected from the femoral artery 1, 2, 3, 5, 10, 30, 60, and 120 minutes after tracer administration for analysis of fluorine-18 metabolites in plasma. For Rat 10, the common bile duct was canaliculated (Intramedic^{TM}, BD, PE 10 catheter, length 20 cm, inner diameter 0.28 cm) and samples were collected 0-15, 15-30, 30-45, 45-60, 60-75, 75-90, and 90-105 min after tracer administration for analysis of fluorine-18 metabolites in bile. Both plasma and bile samples were fractionated by reverse-phase HPLC (20 min run with collection of 1 fraction/min). The column was a Phenomenex® Luna® 10 µ C18(2) 100A (10 µm, 250x10 mm) with an isocratic eluent of 70% acetonitrile in aqueous 1 mM NH$_4$OAc (pH 3.0; adjusted with glacial acetic acid) and a flow of 3 mL/min. With these conditions, non-metabolized [^{18}F]FBCGly elutes in fractions 10–12. Each collected faction was measured in a well counter (Packard Biosciences).

2.4 In vitro stability test of FBCGly towards enzymatic de-conjugation by Cholylglycine Hydrolase

The possible de-conjugation of FBCGly, cholylsarcosine, and cholylglycine, catalyzed by Cholylglycine Hydrolase, was investigated *in vitro* in two separate experiments using previously described conditions [30]: to a solution of the unlabeled conjugated bile acid (2 µM) in 0.25 M aqueous NaOAc buffer (0.4 mL; pH 5.6) were added 1.85% aqueous EDTA (0.2 mL), 0.87% aqueous mercaptoethanol (0.2 mL), and an aqueous suspension of Cholylglycine Hydrolase (0.2 mg; 0.2 mL). The mixture was incubated at 37 $^{\circ}$C and samples were collected after 5 min, 15 min, 30 min, 1 hour, 2 hours, and 24 hours. The samples were analyzed by LC-MS as described for [^{18}F]FBCGly and the relative amount of de-conjugation was determined from the amount of cholic acid formed.

3. Results

3.1 Radiochemistry

The developed radiosynthesis provided [^{18}F]FBCGly (0.4–1.1 GBq) with a non-decay corrected radiochemical yield of 1.0% ± 0.3% (mean ± SD; n = 12; based on delivered [^{18}F]fluoride) and a radiochemical purity of 96% ± 1% (mean ± SD; n = 12) (Fig. 2a and 2b). No free [^{18}F]fluoride was detected in the formulation of [^{18}F]FBCGly (Supplementary Material). The molar radioactivity of [^{18}F]FBCGly was determined to 13 ± 2 GBq/μmol (mean ± SD; n = 4). In its formulation, a clear solution (pH 7–8) without any visible particles, [^{18}F]FBCGly showed no alterations in chemical or radiochemical purity for up to 4 h after the end of synthesis. The first step of the radiosynthesis proceeded with a non-decay corrected yield of approximately 20% to give [^{18}F]FBA with a radiochemical purity of ≥90% (Fig. 1; step i), while the condensation of [^{18}F]FBA to glycine methyl ester followed by *in situ* reduction of the intermediate Schiff base by NaBH$_4$ (steps ii and iii) proceeded with full conversion of [^{18}F]FBA to give 75% ± 4% (mean ± SD; n = 5) [^{18}F]FBGly-ME. The remaining radioactivity was found as 4-[^{18}F]fluorobenzylalcohol (16% ± 8%; n = 5) and an unknown species (9% ± 6%; n = 5) (Table S1 in Supplementary Material). The *in situ* coupling of [^{18}F]FBGly-ME with cholic acid (Fig. 1; step iv) proceeded to give [^{18}F]FBCGly-ME with a conversion of 62% ± 8% (mean ± SD; n = 6) (Table S1). Only [^{18}F]FBGly-ME reacted with cholic acid during this step; the by-products 4-[^{18}F]fluorobenzylalcohol and the unknown species were unreactive. Typical HPLC chromatograms are presented in Fig. 2c and 2d to illustrate the formation of reaction intermediates and by-products during steps ii-iv of the radiosynthesis of [^{18}F]FBCGly. The final step, basic hydrolysis of [^{18}F]FBCGly-ME (Fig. 1; step v), proceeded with full conversion. To improve the overall radiochemical yield, we tested the effect of time by using 3 timer longer reaction times for steps ii–iv and included HPLC purification of [^{18}F]FBA and [^{18}F]FBCGly-ME. However, these modifications did not significantly improve the overall non-decay corrected radiochemical yield of the radiosynthesis (3% ± 1%; mean ± SD; n = 3) or the radiochemical purity of [^{18}F]FBCGly (97% ± 1%; mean ± SD; n = 3).

3.2 In vivo PET/MR and metabolite studies

Fig. 3 shows the result of a dynamic PET/MR recording after i.v. injection of [^{18}F]FBCGly in an untreated rat (Rat 1). [^{18}F]FBCGly was rapidly taken up into liver tissue within one minute after tracer administration followed by secretion into the bile duct within 2 minutes (Fig. 3a and 3b). The tracer subsequently dispersed into the small intestine and, about 20 min after administration, it had cleared liver tissue and bile duct and was visible only in the intestine (and in some cases also the stomach; presumably the result of relaxation of the pyloric valve caused by the anesthesia) (Fig. 3c and 3d). EHC of [^{18}F]FBCGly was observed as the reappearance of radioactivity in liver tissue, bile duct, and duodenum approximately 55 min after tracer administration (Fig. 3e). No radioactivity was observed in the kidneys. Fig. 4 shows grouped time courses of radioactivity concentrations of [^{18}F]FBCGly measured by PET in untreated rats (Rats 1–3), in rats treated with cholyltaurine (Rats 4 and 5), or in rats treated with rifampicin (Rats 6 and 7). Time courses for the individual animals are presented in Fig. S1 (Supplementary Material). In the liver tissue and bile duct of the untreated rats, the radioactivity concentrations peaked at 2 and 3 min, respectively, with a peak concentration in the bile duct approximately 15 times higher than that in liver tissue (Fig. 4). The radioactivity concentrations subsequently decreased rapidly to low concentrations within 25–30 min, and then increased again after 40–60 min in liver tissue and, shortly after, in bile duct as the result of EHC. In rats treated with cholyltaurine and rifampicin (Fig. 4), the biliary secretion of [^{18}F]FBCGly was significantly inhibited as observed by a delayed disappearance of tracer from liver tissue and reduced radioactivity concentrations in the bile duct.

The analysis of plasma and bile samples (Rats 8–10) showed no fluorine-18 metabolites for up to two hours after injection of [^{18}F]FBCGly, and confirmed that the second increase in bile radioactivity concentration was due to [^{18}F]FBCGly (Fig. 5a and 5b; the delayed decrease of the radioactivity concentration in the collected bile compared to that measured by PET is due to dispersion of the tracer in the sampling catheter).

3.3 In vitro stability test of FBCGly towards enzymatic de-conjugation by Cholylglycine Hydrolase

Cholylglycine Hydrolase catalyzed the hydrolysis of cholylglycine by 96% within 5 min at 37 ^{o}C, while only 4% of cholylsarcosine was hydrolyzed after 24 hours. These results are similar to what has previously been reported [30]. Under the same conditions, no hydrolysis of FBCGly was observed for up to 24 hours.

4. Discussion

We have developed a radiosynthesis of N-(4-[18F]fluorobenzyl)cholylglycine ([18F]FBCGly), a novel fluorine-18 labeled bile acid conjugate derived from endogenous cholylglycine. The radiosynthesis is based on reductive alkylation of glycine with 4-[18F]fluorobenzaldehyde followed by coupling to endogenous cholic acid. The radiosynthesis provides [18F]FBCGly with sufficiently high radiochemical purity and radioactivity amount for preclinical evaluation of the tracer, although the radiochemical yield needs to be improved for translation of [18F]FBCGly to clinical studies. In the present study, we showed that [18F]FBCGly does not metabolize *in vivo* in rats; only non-metabolized tracer was observed in plasma and bile for up to two hours after i.v. injection of the tracer. In addition, we showed that FBCGly is stable towards de-conjugation (for up to 24 h) by Cholylglycine Hydrolase from *Clostridium perfringens* (*C. welchii*), a bacteria commonly found in the human intestinal microflora. De-conjugation is the first step in the intestinal biotransformation of endogenous bile acid conjugates and occurs increasingly from the distal small intestine to the terminal ileum and, particularly, in the colon [1, 10]. Indeed, as shown here and elsewhere [30], Cholylglycine Hydrolase rapidly de-conjugates endogenous cholylglycine. The stability of FBCGly towards de-conjugation is believed to be due to the additional substituent, 4-fluorobenzyl, on the nitrogen atom. A similar stability was observed for cholylsarcosine (*N*-methyl-cholylglycine), which has a methyl group on the nitrogen atom, and for *N*-benzyl-ursodeoxycholyltaurine, a derivative of endogenous ursodeoxycholyltaurine with an unsubstituted benzyl group on the nitrogen atom [31, 32]. Thus, [18F]FBCGly does not undergo hepatic or intestinal metabolism on the timescale of the present PET studies.

The dynamic PET/MR studies in rats revealed that, similar to endogenous bile acid conjugates and [11C]cholylsarcosine [20], [18F]FBCGly is rapidly taken up by the liver, secreted into bile, and onwards into the small intestine. The EHC of [18F]FBCGly is observed as the reappearance of the tracer in liver tissue, bile duct and duodenum measured by PET and analysis of bile samples. [18F]FBCGly did not reappear in arterial plasma after its initial clearance, which is in accordance with the EHC of endogenous bile acid conjugates

that return from the small intestine to the liver via portal venous circulation [10]. We expect that the intestinal absorption of [^{18}F]FBCGly occurs beyond duodenum, since the time between the initial peak and the second increase in radioactivity concentration in liver tissue and bile duct is too long (more than 40 minutes) to be explained solely by duodenal absorption of the tracer. In addition, the EHC of [^{18}F]FBCGly sometimes appeared as a relatively narrow peak and sometimes as a very broad peak in the time courses of radioactivity concentrations measured by PET (Fig. S1 in Supplementary Material). We attribute this observation to a normal variation in intestinal mobility and a gradual absorption of [^{18}F]FBCGly during its passage through the small intestine. In some cases (Rat 2 and Rat 6 in Fig. S1), we observed a total of three increments in the radioactivity concentrations in liver tissue and bile duct each 50–60 minutes apart. This observation indicates that [^{18}F]FBCGly circulates continuously, similar to endogenous bile acid conjugates, which are efficiently reabsorbed in the small intestine by more than 90% for each cycle [8, 9].

Because [^{18}F]FBCGly is a conjugated bile acid derivative, it is likely to be fully ionized at physiological pH and, hence, requires active transport to cross hepatocyte and enterocyte membranes during its EHC [10, 33]. Due to the high transport capacity of conjugated bile acids in the liver and the small intestine, the molar radioactivity of [^{18}F]FBCGly (13 ± 2 GBq/μmol) is not a significant factor in terms of *in vivo* transport studies. In the hepatocytes, two transporter proteins should be considered in particular for the transport of [^{18}F]FBCGly across the canalicular membrane: the BSEP, which constitutes the major driving force for the secretion of conjugated bile acids from hepatocytes into bile, and the less specific Multidrug Resistance Protein 2 (MRP2). To investigate which of these two proteins are likely to transport [^{18}F]FBCGly, we used rifampicin as inhibitor, because it is known to directly *cis*-inhibit BSEP without inhibiting MRP2 in rats [34]. We found that rifampicin significantly inhibited the biliary secretion of [^{18}F]FBCGly. In accordance with this, endogenous cholyltaurine, which is transported to a major extent by rat BSEP [34], also inhibited the biliary secretion of [^{18}F]FBCGly significantly. Thus, the BSEP is likely to be a major transporter of [^{18}F]FBCGly from hepatocytes into bile, although other canalicular transporter proteins may also be involved. The results also

14

indicate that cholyltaurine inhibits the transport of [18F]FBCGly across the intestinal membrane as observed by a delayed EHC of the tracer in rats treated with cholyltaurine (more than 70 min recirculation time) compared to untreated rats and rats treated with rifampicin (40–60 min recirculation time). This finding suggests that [18F]FBCGly and cholyltaurine compete for one or more of the same transporter proteins in the enterocyte membranes. To what extent individual transporter proteins are involved in the transcellular transport of [18F]FBCGly in hepatocytes and enterocytes remain however to be investigated.

5. Conclusion

We have developed a radiosynthesis of a novel fluorine-18 labeled bile acid derivative, *N*-(4-[^{18}F]fluorobenzyl)cholylglycine ([^{18}F]FBCGly), and shown by dynamic PET/MR in rats that [^{18}F]FBCGly undergoes continuous EHC without metabolizing. To the best of our knowledge, [^{18}F]FBCGly is the first PET tracer shown to undergo EHC. Under normal conditions, [^{18}F]FBCGly is subject to a rapid transhepatic transport, resulting in high concentrations of the tracer in bile, but it is inhibited by rifampicin and endogenous cholyltaurine, which indicate that the BSEP is likely to be involved in the secretion of [^{18}F]FBCGly from hepatocyte into bile. We envision that [^{18}F]FBCGly PET can be used as tool for non-invasive *in vivo* investigations of the pathological mechanisms of diseases that affect the EHC and of drugs inhibiting hepatic and intestinal transport of conjugated bile acid.

Acknowledgement

Figure Legends

Fig. 1. Radiosynthesis of [^{18}F]FBCGly. Reagents and conditions: i) [^{18}F]KF-K222, dimethylsulfoxide, 105 °C, 10 min; ii) glycine methyl ester hydrochloride, triethylamine, dimethylsulfoxide, 60 ^{o}C, 10 min; iii) sodium borohydride, dimethylsulfoxide, 25 ^{o}C, 5 min; iv) cholic acid, triethylamine, diethyl phosphoryl cyanide, dimethylsulfoxide, 60 ^{o}C, 10 min; v) purification, then 0.25 M NaOH, room temperature, 10 min, then neutralization with aqueous 70 mM NaH$_2$PO$_4$.

Fig. 2. Typical HPLC chromatograms recorded during radiosynthesis of [^{18}F]FBCGly: (a) shows a radiochromatogram of purified [^{18}F]FBCGly ready for injection (HPLC sample collected after step v in Fig. 1); (b) shows radio- (full line) and UV- (dotted line) chromatograms of [^{18}F]FBCGly co-injected with unlabeled FBCGly for identification of the tracer; (c) shows radiochromatograms of the conversion of [^{18}F]FBA (dotted line) into [^{18}F]FBGly-ME (full line; crude sample collected after step iii in Fig. 1); (d) shows a radiochromatogram of the *in situ* conversion of crude [^{18}F]FBGly-ME into [^{18}F]FBCGly-ME (sample collected after step iv in Fig. 1).

Fig. 3. Coronal PET/MR images of the time course of distribution of [^{18}F]FBCGly recorded as mean values (MBq/mL) in the time intervals indicated during the 120-min PET scan of Rat 1 (240 g; anesthetized with 2% isoflurane) after i.v. bolus injection of tracer (28 MBq). All images are of the same slice.

Fig. 4. Time courses of radioactivity concentrations in liver tissue and bile duct (dynamic PET/MR) after i.v. bolus injection of [^{18}F]FBCGly (19–33 MBq) in untreated rats (controls; Rats 1–3; n = 3), rats treated with cholyltaurine (Rats 4 and 5; n = 2), and rats treated with rifampicin (Rats 6 and 7; n = 2). The insets show the first 30 minutes of the curves. The data is represented as mean (SD). %ID = percent of injected dose. Time courses for the individual animals are presented in Supplementary Material.

Fig. 5. Results from metabolite analysis of (a) arterial plasma and (b) bile samples collected after i.v. bolus injection of [^{18}F]FBCGly in Rat 8 (32 MBq) and Rat 10 (35 MBq), respectively. The radioactivity is decay corrected to the time of injection. Fractions 10–12 correspond to non-metabolized [^{18}F]FBCGly.

References

[1] Frisch K, Hofmann AF. Biliary secretion. In: Keiding S, Sørensen M, editors. Functional Molecular Imaging in Hepatology. Sharjah, UAE: Bentham Science Publishers; 2012, p. 49–75.

[2] Hofmann AF, Hagey LR. Key discoveries in bile acid chemistry and biology and their clinical applications: history of the last eight decades. J Lipid Res 2014;55:1553–95.

[3] Lefebvre P, Cariou B, Lien F, Kuipers F, Staels B. Role of bile acids and bile acid receptors in metabolic regulation. Physiol Rev 2009;89:147–91.

[4] Hofmann AF. Chemistry and enterohepatic circulation of bile acids. Hepatology 1984;4:4S–14S.

[5] Pellicoro A, Faber KN. The function and regulation of proteins involved in bile salt biosynthesis and transport. Aliment Pharmacol Ther 2007;26:149–60.

[6] Kosters A, Karpen SJ. Bile acid transporters in health and disease. Xenobiotica 2008;38:1043–71.

[7] Stieger B. The role of the sodium-taurocholate cotransporting polypeptide (NTCP) and of the bile salt export pump (BSEP) in physiology and pathophysiology of bile formation. In: Fromm MF, Kim RB, editors. Drug transporters Handbook of experimental pharmacology 201. Berlin Heidelberg: Springer-Verlag; 2011, p. 205–59.

[8] Dawson PA. Role of the intestinal bile acid transporters in bile acid and drug disposition. In: Fromm MF, Kim RB, editors. Drug transporters, Handbook of experimental pharmacology 201. Berlin Heidelberg: Springer-Verlag; 2011, p. 169–203.

[9] Dawson PA, Karpen SJ. Intestinal transport and metabolism of bile acids. J Lipid Res 2015;56:1085–99.

[10] Hofmann AF. The enterohepatic circulation of bile acids in mammals: form and functions. Front Biosci (Landmark Ed) 2009;14:2584–98.

[11] Roberts MS, Magnusson BM, Burczynski FJ, Weiss M. Enterohepatic circulation. Physiological, pharmacokinetic and clinical implications. Clin Pharmacokinet 2002;41:751–90.

[12] Dawson PA. Roles of ileal ASBT and OSTα–OSTβ in regulating bile acid signaling. Dig Dis 2017;35:261–6.

[13] Wagner M, Trauner M. Recent advances in understanding and managing cholestasis. F1000Research 2016;5(F1000 Faculty Rev):705.

[14] Wenninger LMdB, Beuers U. Bile salts and cholestasis. Dig Liver dis 2010;42:409–18.

[15] Mottacki N, Simrén M, Bajor A. Review article: bile acid diarrhoa - pathogenesis, diagnosis and management. Aliment Pharmacol Ther 2016;43:884–98.

[16] Neyt S, Vliegen M, Verreet B, Lombaerde SD, Braeckman K, Vanhove C, et al. Synthesis, in vitro and in vivo small-animal SPECT evaluation of novel technetium labeled bile acid analogues to study (altered) hepatic transporter function. Nucl Med Biol 2016;43:642–9.

[17] Anelli PL, Lattuada L, Lorusso V, Lux G, Morisetti A, Morosini P, et al. Conjugates of gadolinium complexes to bile acids as hepatocyte-directed contrast agents for magnetic resonance imaging. J Med Chem 2004;47:3629–41.

[18] Vivian D, Cheng K, Khurana S, Xu S, Dawson PA, Raufman J-P, et al. Design and evaluation of a novel trifluorinated imaging agent for assessment of bile acid transport using fluorine magnetic resonance imaging. J Pharm Sci 2014;103:3782–92.

[19] Felton J, Cheng K, Said A, Shang AC, Xu S, Vivian D, et al. Using multi-fluorinated bile acids and in vivo magnetic resonance imaging to measure bile acid transport. J Vis Exp 2016;117:e54597.

[20] Frisch K, Jakobsen S, Sørensen M, Munk OL, Alstrup AKO, Ott P, et al. [N-Methyl-^{11}C]cholylsarcosine, a novel bile acid tracer for PET/CT of hepatic excretory function: radiosynthesis and proof-of-concept studies in pigs. J Nucl Med 2012;53:772–8.

[21] Schacht AC, Sørensen M, Munk OL, Frisch K. Radiosynthesis of N-^{11}C-methyl-taurine–conjugated bile acids and biodistribution studies in pigs by PET/CT. J Nucl Med 2016;57:628–33.

[22] Jia L, Dawei J, Hu P, Li X, Shi H, Cheng D, et al. Synthesis and evaluation of ^{18}F-labeled bile acid compound: a potential PET imaging agent for FXR-related diseases. Nucl Med Biol 2014;41:495–500.

[23] Chong H-S, Chen Y, Kang CS, Sun X, Wu N. Novel ^{64}Cu-radiolabeled bile acid conjugates for targeted PET imaging. Bioorg Med Chem Lett 2015;25:1082–5.

[24] Testa A, Dall'Angelo S, Mingarelli M, Augello A, Schweiger L, Welch A, et al. Design, synthesis, in vitro characterization and preliminary imaging studies on fluorinated bile acid derivatives as PET tracers to study hepatic transporters. Bioorg Med Chem 2017;25:963–76.

[25] Sørensen M, Munk OL, Ørntoft NW, Frisch K, Andersen KJ, Mortensen FV, et al. Hepatobiliary secretion kinetics of conjugated bile acids measured in pigs by ^{11}C-cholylsarcosine PET. J Nucl Med 2016;57:961–6.

[26] Lombaerde SD, Neyt S, Kersemans K, Verhoeven J, Devisscher L, Vlierberghe HV, et al. Synthesis, in vitro and in vivo evaluation of 3β-[^{18}F]fluorocholic acid for the detection of drug-induced cholestasis in mice. PLoS One 2017;12:e0173529.

[27] Ørntoft NW, Munk OL, Frisch K, Ott P, Keiding S, Sørensen M. Hepatobiliary transport kinetics of the conjugated bile acid tracer ^{11}C-CSar quantified in healthy humans and patients by positron emission tomography. J Hepatol 2017;67:321–7.

[28] Dickson I. Liver: PET for bile transport kinetics. Nat Rev Gastroenterol Hepatol 2017;14:260–1.

[29] Åberg O, Pisaneschi F, Smith G, Nguyen Q-D, Stevens E, Aboagye EO. ^{18}F-labelling of a cyclic pentapeptide inhibitor of the chemokine receptor CXCR4. J Fluorine Chem 2012;135:200–6.

[30] Batta AK, Salen G, Shefer S. Substrate specificity of cholylglycine hydrolase for the hydrolysis of bile acid conjugates. J Biol Chem 1984;259:15035–9.

[31] Frick E, Hagey LR, Schteingart CD, Ton-Nu H-T, Bolder U, Cerrè C, et al. Metabolism and enterohepatic circulation of a new conjugated bile acid analogue: ursodeoxycholyl-*N*-benzyltaurine [abstract]. Hepatology 1995;22(suppl 4):320A.

[32] Frick E, Hagey LR, Schteingart CD, Ton-Nu H-T, Bolder U, Hofmann AF. Metabolism, toxicity, and transport properties in hamsters of ursodeoxycholyl-*N*-benxyl-taurine, a new conjugate of ursodeoxycholic acid [abstract]. Gastroentelogy 1996;110(suppl):A1191.

[33] Hofmann AF, Hagey LR. Bile acids: chemistry, pathochemistry, biology, pathobiology, and therapeutics. Cell Mol Life Sci 2008;65:2461–83.

[34] Stieger B, Fattiger K, Madon J, Kullak-Ublick GA, Meier PJ. Drug- and estrogen-Induced cholestasis through inhibition of the hepatocellular bile salt export pump (Bsep) of rat liver. Gastroentelogy 2000;118:422–30.
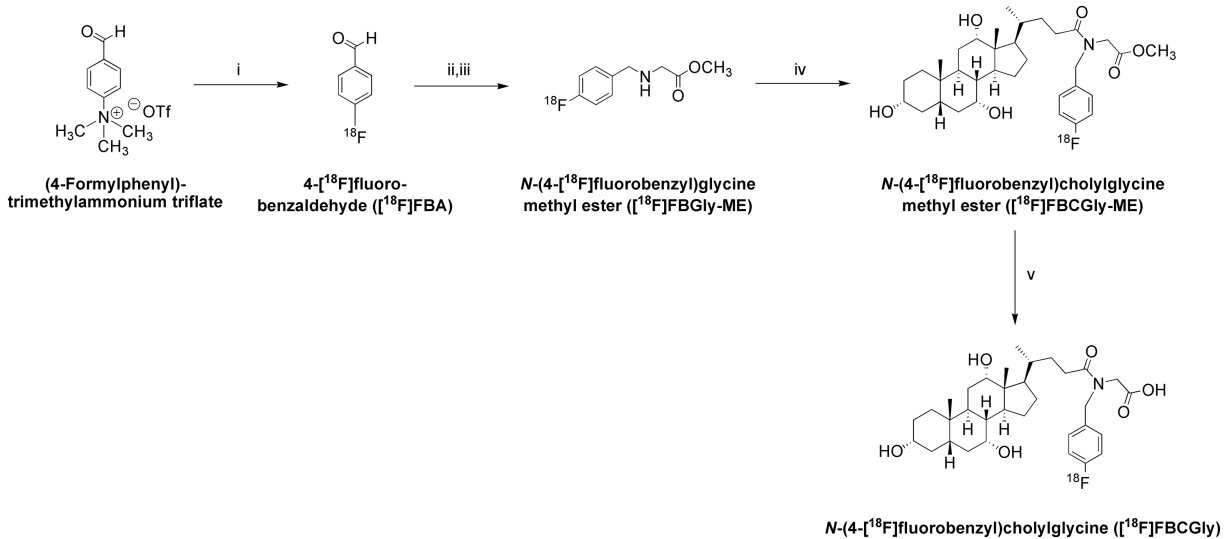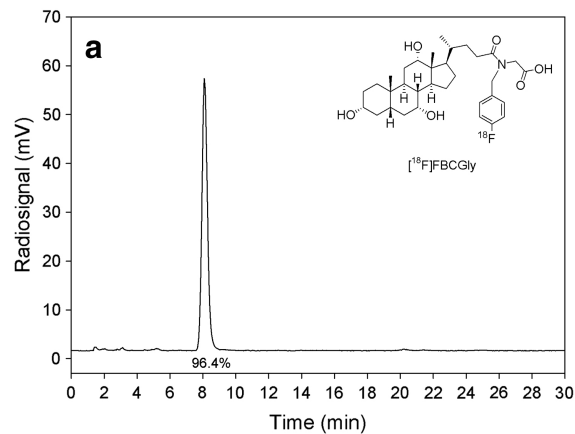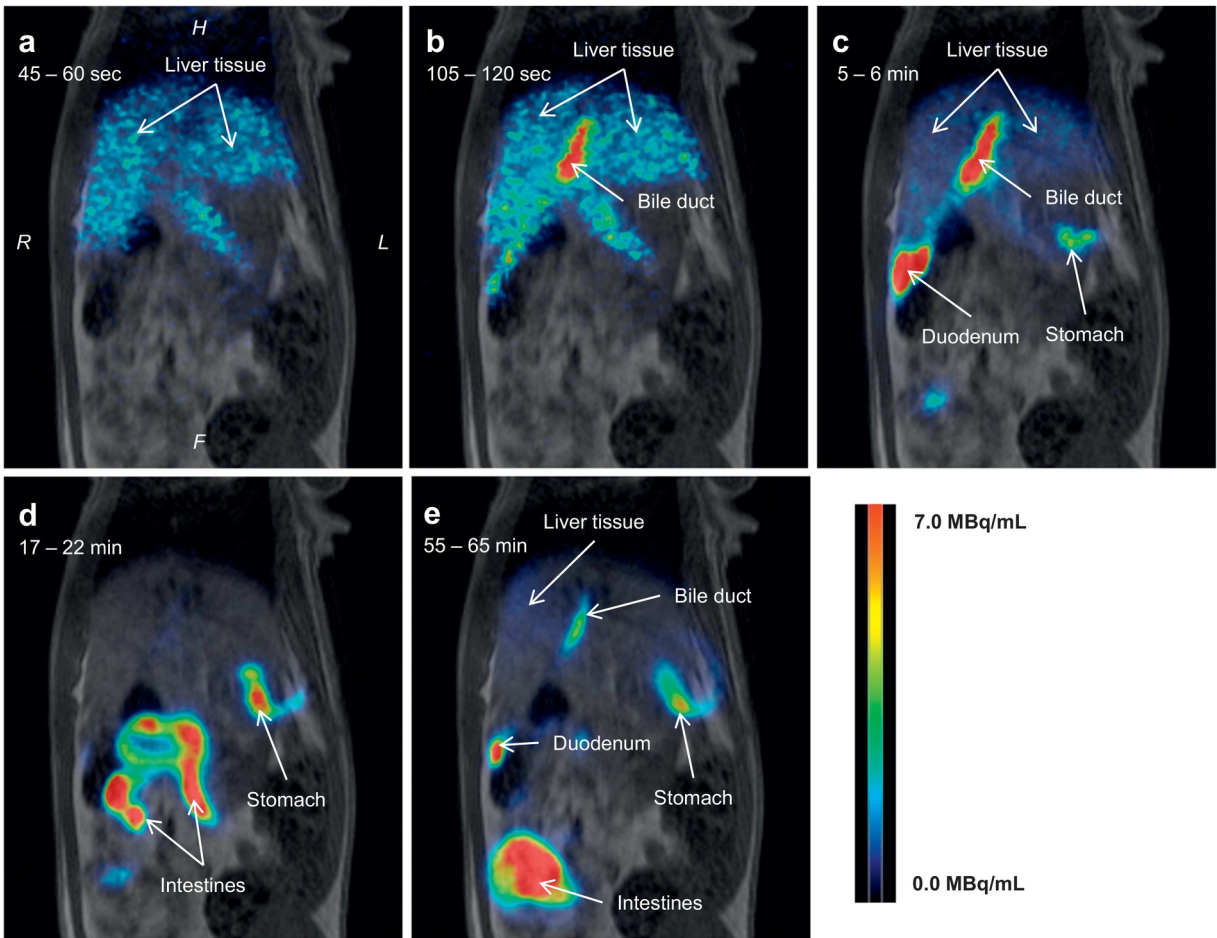
Figure 1
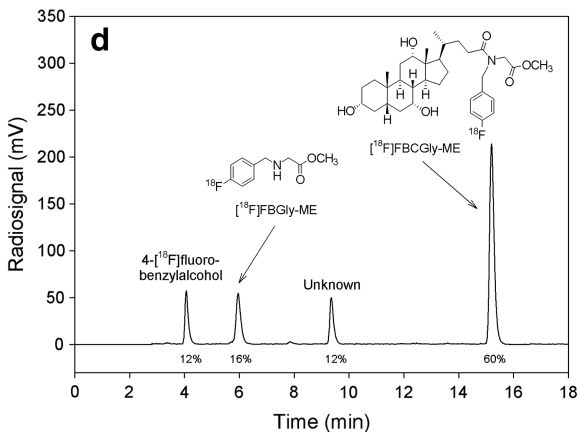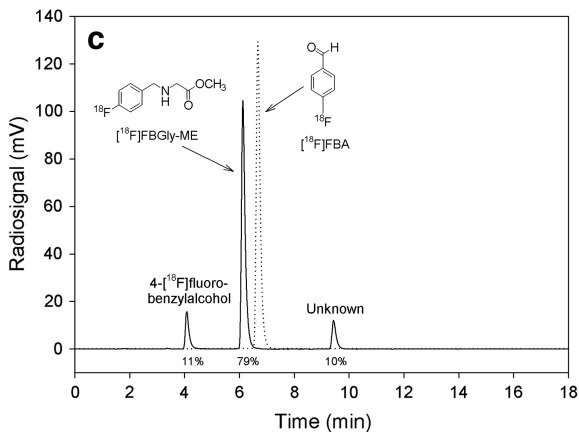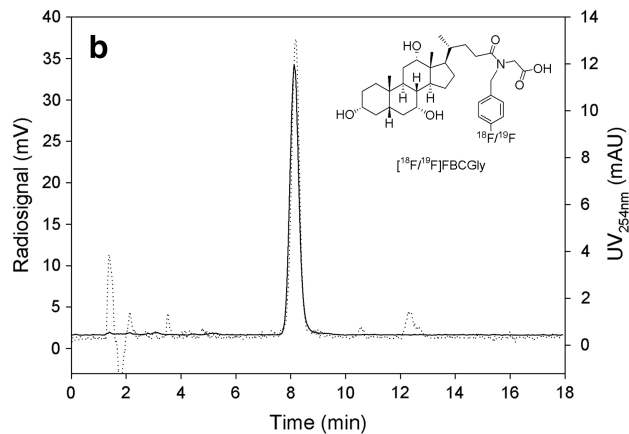
Figure 2

Figure 3

Figure 4

Figure 5